

# SaBOX/Copper Catalysts for Highly Syndio-Specific Atom Transfer Radical Polymerization of Methyl Methacrylate

Xiao-Yan Wang,<sup>†,‡</sup> Xiu-Li Sun,<sup>†</sup> Feng Wang,<sup>†</sup> and Yong Tang<sup>\*,†,‡</sup>

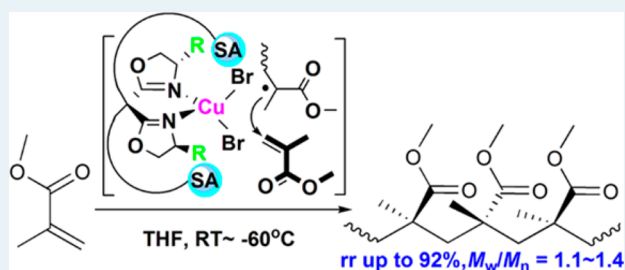
<sup>†</sup>State Key Laboratory of Organometallic Chemistry, Shanghai Institute of Organic Chemistry, Chinese Academy of Sciences, 345 Lingling Lu, Shanghai 200032, China

<sup>‡</sup>Collaborative Innovation Center of Chemical Science and Engineering, Tianjin 300071, China

## Supporting Information

**ABSTRACT:** SaBOX/copper catalysts have been developed, giving a highly syndio-specific (triad syndiotacticity *rr* over 90%) and well-controlled (molecular weight distribution  $\mathcal{D} = 1.1\text{--}1.4$ ) atom transfer radical polymerization (ATRP) of methyl methacrylate. The substituents on the bisoxazoline (BOX) scaffold significantly affect the polymerization rate, molecular weight, and stereoselectivity. The side arms installed on the bridge carbon of BOX have been proven to strongly influence both the activity of the catalyst and the tacticity of the resulting polymers, paving an alternative way for the control of stereoselectivity in ATRP. X-ray structural determination and the Eyring approach were employed to obtain insights into the scaffold and side arm effects on catalyst performance.

**KEYWORDS:** catalyst, side armed bisoxazoline (SaBOX), atom transfer radical polymerization (ATRP), stereospecificity, side arm strategy



## INTRODUCTION

Since the pioneering work by Matyjaszewski et al.,<sup>1-4</sup> atom transfer radical polymerization (ATRP) has proven to be a powerful tool for synthesis of polymers with almost perfect control over molecular weight (MW) and topology.<sup>5-19</sup> However, its stereochemical control has been considered a great challenge, especially for simple monomers such as methyl methacrylate (MMA), because of the planar nature of the chain-end carbon radical.<sup>20-33</sup> To date, the simultaneous control of MW and chain microstructure during ATRP is still one of the most challenging goals for polymer chemists.<sup>23-26</sup> Although anionic and coordinative polymerization of MMA proves to be stereocontrolled by organometallic catalysts,<sup>34-38</sup> all studies so far showed that stereochemistry is difficult to control in ATRP and transition metal catalysts have little or no influence on polymer tacticity for ATRP. This was attributed to a remote control in which the radical species diffuse away from the “counter radical” (transition metal center) prior to subsequent monomer addition.<sup>27-29</sup> In addition, compared with typical anionic polymerization or coordination polymerization, ATRP can provide well-defined polymers with more diverse functionality and architecture as well as copolymers with a variation of repeating units over a large range under less stringent reaction conditions.<sup>1-19</sup> Therefore, finding a new way to control the polymer tacticity based on ATRP, which would be potentially useful in the precise synthesis of polymers with novel topology and application, is quite important.

Early studies showed that the polymers obtained by ATRP with various achiral catalysts have almost the same tacticities

compared to the tacticities of those obtained in conventional free radical polymerizations.<sup>1-4</sup> Subsequently, several chiral complexes have been prepared for ATRP to exert stereochemical control.<sup>30-33</sup> Nevertheless, the resultant polymers showed a stereochemistry similar to those obtained in ATRP with achiral catalysts. Moreover, a broader MW distribution was observed in some of these cases. To date, the tuning of the stereospecificity in ATRP by only a catalyst is still an unsolved puzzle in the field of polymer chemistry.<sup>20-33</sup> In the past several years, we have become interested in conquering this problem. On the basis of an elegant catalytic system for activator generated by electron transfer (AGET) ATRP with zero-valent copper as the reducing agent,<sup>39-41</sup> very recently, we demonstrated that a newly designed catalyst based on a side arm strategy is highly active for ATRP of MMA, allowing a lower polymerization temperature and making the catalyst capable of mediating ATRP of MMA in a highly syndio-specific manner, while keeping satisfactory control over MW. Herein, we report the preliminary results.

## RESULTS AND DISCUSSION

**Effects of the BOX Scaffold on the Polymerization of MMA.** Our study was initiated by using elemental copper as the reducing agent and 2-bromopropionitrile (BPN) as the initiator in the bisoxazoline (BOX)/CuBr<sub>2</sub>-based catalytic system for

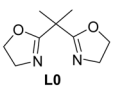
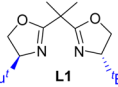
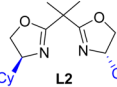
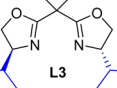
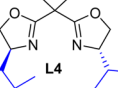
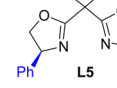
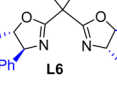
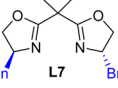
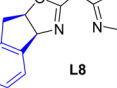
Received: April 4, 2017

Revised: May 31, 2017

Published: June 8, 2017

AGET ATRP of MMA. We first investigated the most common BOXs as ligands for the polymerization of MMA in tetrahydrofuran (THF) at room temperature for 12 h. As shown in Table 1, the substituents on BOX scaffolds obviously

**Table 1. Effects of the BOX Scaffold on AGET ATRP of MMA<sup>a</sup>**

 Conv. 75% rr 68% $M_n$ 11.9 X 10 <sup>3</sup> PDI 1.1	 Conv. 45% rr 72% $M_n$ 19.2 X 10 <sup>3</sup> PDI 1.3	 Conv. 22% rr 71% $M_n$ 17.4 X 10 <sup>3</sup> PDI 1.2
 Conv. 40% rr 71% $M_n$ 26.0 X 10 <sup>3</sup> PDI 1.3	 Conv. 48% rr 71% $M_n$ 16.8 X 10 <sup>3</sup> PDI 1.2	 Conv. 35% rr 72% $M_n$ 37.3 X 10 <sup>3</sup> PDI 1.5
 Conv. 38% rr 72% $M_n$ 15.3 X 10 <sup>3</sup> PDI 1.2	 Conv. 45% rr 72% $M_n$ 20.1 X 10 <sup>3</sup> PDI 1.3	 Conv. 59% rr 72% $M_n$ 9.9 X 10 <sup>3</sup> PDI 1.1

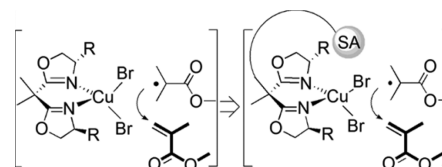
<sup>a</sup>Conditions: 200:2:1:2:4 MMA:BPN:CuBr<sub>2</sub>:ligand:Cu(0) ratio, THF used as the solvent (50%  $V_{total}$ ), 25 °C, 12 h. Monomer conversion (Conv.) was measured by <sup>1</sup>H nuclear magnetic resonance. Number-average molecular weight ( $M_n$ ) and polydispersity indices (PDI) determined by gel permeation chromatography at 25 °C in THF vs narrow PMMA standards, PDI ( $\bar{D}$ ) =  $M_w/M_n$ . Triad syndiotacticity (rr) measured by <sup>1</sup>H nuclear magnetic resonance in CDCl<sub>3</sub> and estimated according to a commonly employed literature method (General Information in the Supporting Information).<sup>34,35,42,43</sup>

affect the polymerization rate. Compared with all the chiral ligands, unsubstituted achiral BOX L0 is more active under the current conditions, giving the highest conversion of 75% and exhibiting excellent control over MW (molecular weight distribution  $\bar{D}$  = 1.1). Chiral Cy-BOX L2 yielded the lowest conversion of 22%, and other chiral ligands (L1 and L3–L7) furnished only moderate conversions of 35–48%. Besides, the MW distributions were slightly broadened ( $\bar{D}$  = 1.2–1.5). Indane-BOX L8 gave a significantly improved conversion (59%) and a narrow MW distribution ( $\bar{D}$  = 1.1). It is further noteworthy that BOX ligands that led to higher activity also exhibited better control of MW. More importantly, substituted BOXs exhibited a stereoselectivity slightly better than that of unsubstituted L0 (triad syndiotacticity rr of ~72% vs 68%), probably because of the extremely open microenvironment around the metal center with L0 as the ligand. These results suggest that the catalyst might influence the microstructure of PMMA, encouraging us to further explore this question.

**Side Arm Effect in SaBOX/Copper-Mediated Polymerization of MMA.** As mentioned above, the catalyst is considered to exert barely any influence on stereocontrol; therefore, the stereoselectivity of ATRP is mainly controlled by the chain end.<sup>23–26</sup> In the past decade, we successfully developed a side arm strategy for the design of organometallic catalysts that can be applied in asymmetric catalysis.<sup>44–50</sup> During these studies, it was found that the side arm installed on the bridge carbon of BOX could greatly enhance the reaction speed and enantioselectivity in a number of BOX/metal-catalyzed reactions related to the remote control of enantioselectivity.<sup>44–50</sup> Thus, we tried to extend this strategy to ATRP for stereochemical control and envisioned that the

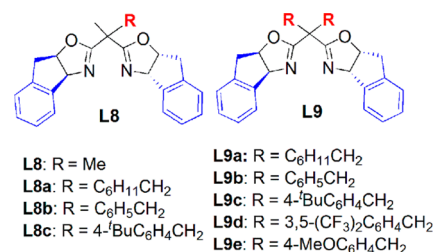
pendant group installed on the bridge carbon could also fine-tune the conformations of the species involved in the radical addition step, impelling the ligand to affect the stereoselectivity of MMA polymerization (Scheme 1). On the basis of this

**Scheme 1. Catalyst Design for the Syndio-Specific ATRP of MMA**



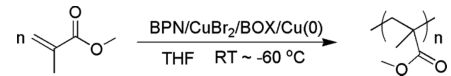
assumption, combining the experimental result that Indane-BOX L8 gave good conversion and stereoregularity, we designed mono- and bis-side armed SaBOX ligands L8a–c and L9a–e on the basis of the side arm strategy (Scheme 2) to study their potential in stereoselective ATRP of MMA.

**Scheme 2. Side Armed Ligands (SaBOX) for Copper-Mediated AGET ATRP**



As shown in Table 2, when the polymerizations are performed at 0 °C, one pendant group installed on BOX has little effect on the activity and stereoselectivity (entries 3–6). To our delight, a strong side arm effect on the activity and stereoselectivity is observed in the case of bis-side armed SaBOX ligands. When SaBOX L9a was used instead of L0 or L8, conversion increased from 49 to 75% and the rr value was improved from 71 to 78% (entries 2 and 3 vs entry 7). In this case, the MW distribution is very narrow ( $\bar{D}$  = 1.1). When the cyclohexylmethyl group is changed to a benzyl group, the conversion decreased to 40% (entry 8). Further studies showed that the nature and position of the substituents on the benzyl group could not improve the activity (entries 9–11). It is noteworthy that the influence of the ligand (catalyst) on the tacticity increases significantly at lower temperatures (entries 2–20). For instance, at –40 °C, the rr value was 79% in the case in which L0 was employed, while L9a gave 88% rr (entry 15 vs entry 17). When the temperature was decreased to –60 °C, 92% rr was achieved by using L9a. For all we know, this is by far the highest syndiotacticity obtained in ATRP of MMA (entry 20). Besides, a good control over MW distribution was observed in this case.

To further confirm that the catalyst can affect the stereoregularity, we also conducted conventional free radical polymerizations at –20, –40, and –60 °C, initiated by (*n*-Bu)<sub>3</sub>B in the presence of a small amount of oxygen and employing THF as the solvent.<sup>42,43</sup> As shown in Table S1, the rr values are much lower than those achieved in ATRP mediated by a SaBOX (L9a)/copper catalyst at each temperature (75% vs 84%, 77% vs 88%, and 80% vs 92%, respectively),

**Table 2. Syndio-Specific AGET ATRP of MMA Mediated by Copper Catalysts<sup>a</sup>**


entry	L	T (°C)	t (h)	Conv. <sup>b</sup> (%)	$M_n^c$ ( $\times 10^3$ )	$\bar{D}^c$	rr <sup>d</sup> (%)
1	L9a	25	12	93	9.96	1.1	72
2	L0	0	36	55	12.1	1.3	71
3	L8	0	36	49	13.4	1.1	74
4	L8a	0	36	51	13.7	1.2	76
5	L8b	0	36	47	11.1	1.1	74
6	L8c	0	36	36	11.8	1.2	75
7	L9a	0	36	75	12.9	1.1	78
8	L9b	0	36	40	8.90	1.1	75
9	L9c	0	36	35	12.9	1.2	75
10	L9d	0	36	30	10.9	1.2	76
11	L9e	0	36	45	12.4	1.2	75
12	L0	-20	48	39	15.3	1.2	76
13	L8	-20	48	15	14.1	1.3	80
14	L9a	-20	48	45	13.1	1.2	84
15	L0	-40	60	24	17.4	1.2	79
16	L8	-40	60	10	10.7	1.3	83
17	L9a	-40	60	25	15.8	1.2	88
18	L0	-60	72	10	42.6	1.4	82
19	L8	-60	72	trace	—	—	—
20	L9a	-60	72	12	32.8	1.4	92

<sup>a</sup>Conditions: 200:2:1:2:4 MMA:BPN:CuBr<sub>2</sub>:ligand:Cu(0) ratio, THF used as the solvent (50%  $V_{\text{total}}$ ). <sup>b</sup>Monomer conversion measured by <sup>1</sup>H nuclear magnetic resonance. <sup>c</sup>Number-average molecular weights and polydispersity indices determined by gel permeation chromatography at 25 °C in THF vs narrow PMMA standards ( $\bar{D} = M_w/M_n$ ). <sup>d</sup>Triad syndiotacticity (rr) measured by <sup>1</sup>H nuclear magnetic resonance in CDCl<sub>3</sub> and estimated according to a commonly employed literature method (General Information of the Supporting Information).<sup>34,35,42,43</sup>

clearly demonstrating the main effects of the SaBOX/copper catalyst on controlling tacticity.

The physical properties of polymers are often significantly affected by main chain tacticity. Therefore, PMMA samples with different syndiotacticities were analyzed by DSC measurement (Figure 1). As shown by the DSC curves, the  $T_g$  of PMMA regularly shifted to a higher temperature (from 123 to 139 °C) with an increase in rr from 68 to 92%,<sup>51,52</sup> being

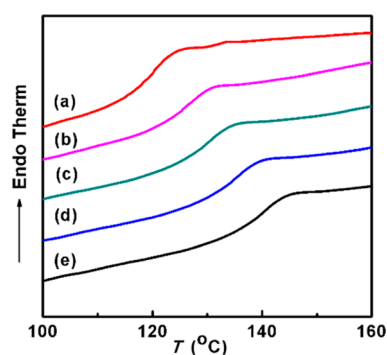


**Figure 1.**  $T_g$  values for PMMA with regularly increasing triad syndiotacticity (rr). (a)  $T_g = 123$  °C, and rr = 68% (Table 1, L0). (b)  $T_g = 126$  °C, and rr = 72% (Table 2, entry 1). (c)  $T_g = 131$  °C, and rr = 78% (Table 2, entry 7). (d)  $T_g = 134$  °C, and rr = 84% (Table 2, entry 14). (e)  $T_g = 139$  °C, and rr = 92% (Table 2, entry 20).

consistent with the tacticity of PMMA determined from <sup>1</sup>H nuclear magnetic resonance (NMR) spectra.<sup>34,35,42,43</sup>

**Evidence for the ATRP Mechanism.** In the current method, 93% conversion in 12 h was achieved during the polymerization conducted at room temperature using L9a as the ligand, which presented a highly efficient polymerization (Table 2, entry 1). A linear first-order kinetic plot and an agreement between the experimental and theoretical MW were proof of a controlled polymerization (Figures S4 and S5). Further study showed that addition of 1.5 equiv of galvinoxyl radical relative to the initiator (BPN) completely inhibits the polymerization. No MMA polymerization occurred within 12 h, which supports the participation of free radicals in the polymerization.<sup>1,2</sup> To analyze the retained chain ends precisely by matrix-assisted laser desorption ionization time-of-flight mass spectrometry, PMMA with a low MW ( $M_n = 3683$ ) was prepared using L9a (Figure S6). The result showed almost completely retained active C–Br chain-end functionalities. This manifests in the fact that the polymerization proceeded in an ATRP manner. Thus, the polymerization presented here demonstrated for the first time that the microstructure of polymers generated through ATRP of MMA can also be tuned by the catalyst only.

**Insight into the Side Arm Effect Based on the Molecular Structure of Catalysts.** Because the key step in ATRP involves a fast and reversible halogen exchange between the metal center and polymer chain end, the coordination environment imposed by ligand is a key factor in this process.<sup>53</sup> Thus, to understand the side arm effects on the stereochemistry, we grew several single crystals of Cu(II) and Cu(I) complexes for X-ray structure determination. As shown in Figure 2 and Figures S7–S12, both of the pendant cyclohexyl

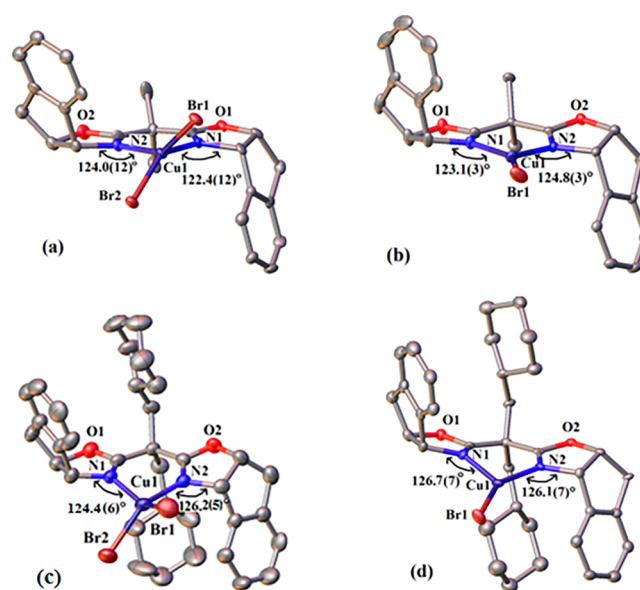


**Figure 2.** Molecular structures of (a) L8/CuBr<sub>2</sub>, (b) L8/CuBr, (c) L9a/CuBr<sub>2</sub>, and (d) L9a/CuBr complexes.

groups in the L9a/CuBr<sub>2</sub> and L9a/CuBr complexes shift toward the copper center, similar to the case for the SaBOX/Cu(II) complexes reported previously.<sup>54</sup> Thus, the introduction of two cyclohexylmethyl side arms (L9a) envelops the upper and lower side of the coordination plane (N1–Cu1–N2), forming a more encapsulated active cavity resulting in strong



steric effects. This is probably the reason why the cyclohexyl groups in **L9a** could enhance the stereoselectivity in the current polymerizations. Interestingly, the dihedral angles around the metal center (C3–N1–Cu1, C13–N2–Cu1 and C1–N1–Cu1, C21–N2–Cu1, respectively) in SaBOX complexes are larger than those of the corresponding Cu(II) and Cu(I) complexes with the parental ligand **L8** (Figure 2 and Figures S9–S12). This indicates that both SaBOX/Cu(II) and SaBOX/Cu(I) complexes possess a wider cavity around the active center, improving fast halogen exchange and explaining well the fact that **L9a** achieved a faster polymerization rate as well as a better MW control compared with those of the parental BOX.

**Further Understanding of Catalyst-Tuned Syndio-Specific ATRP via an Eyring Approach.** As mentioned above, the syndio-selectivity in the polymerization of MMA is temperature-dependent: the lower the reaction temperature, the higher the stereoselectivity. To better understand this observation, an Eyring plot was made and showed a linear dependence of  $\ln(\% r/\% m)$  on the reciprocal temperature for the polymerizations conducted with **L0**, **L8**, and **L9a**, following the modified Eyring approach of eq a (Figure 3 and Figure S13

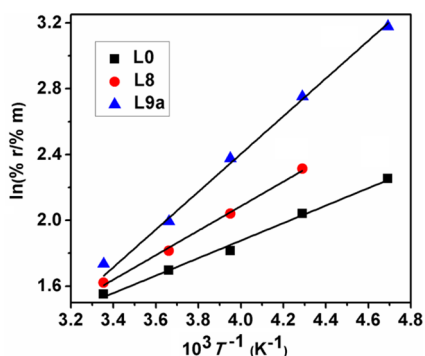


**Figure 3.** Eyring plots for the syndio-specific ATRP of MMA by ligands **L0**, **L8**, and **L9a**, following the modified Eyring approach of the following equations: (a)  $\ln(P) = -(\Delta\Delta H^\ddagger/R)(1/T) + \Delta\Delta S^\ddagger/R$  and (b)  $P = (\% \text{ major isomer})/(\% \text{ minor isomer})$ .

and Table S2), indicating the dominance of enthalpy in the partial selectivity steps compared with entropy in the temperature region from 25 to  $-60$  °C.<sup>55</sup> The different slopes of the three fitting lines represent the energetic barriers for different configurations of species involved in the radical addition step. Apparently, the energetic barriers for polymerizations with different ligands decrease in the following order: **L9a** > **L8** > **L0**. This is consistent with the stereoselectivity for polymerizations using these ligands.

## CONCLUSION

In summary, we have developed a highly syndio-specific (>90% rr) and controlled ATRP of MMA in a common solvent by employing newly designed catalysts. This method provides the first example of tuning the stereochemistry in ATRP of MMA by a catalyst only. The use of the Indane-BOX scaffold is crucial for an enhanced polymerization rate and stereoregularity. This study also demonstrates that the side arm strategy is highly efficient for designing and/or modifying catalysts in stereo-specific ATRP, paving a new way to control the polymer structure in ATRP. The mild polymerization conditions together with well-controlled MW and MW distribution as well as the high syndio-specificity make the current method

potentially useful in the precise synthesis of polymers with a novel topology and application.

## EXPERIMENTAL SECTION

**General AGET ATRP Procedure.** All polymerizations were set up and performed under an atmosphere of oxygen-free dry argon using standard Schlenk line techniques or inside a nitrogen-filled glovebox. In an ampule equipped with a magnetic stirring bar, a mixture of CuBr<sub>2</sub>, ligand, and Cu(0) powder in solvent was stirred at room temperature for 2 h under a nitrogen atmosphere. Then, the catalyst mixture was cooled to a certain temperature for 20 min if necessary. After that, the monomer and initiator were added to the ampule. The ampules were placed at room temperature or cooled in a low-temperature thermostat bath. After the mixture had been stirred for the allotted period of time, an aliquot (0.1 mL) was removed, and the reaction was quenched with CDCl<sub>3</sub> (0.5 mL). Conversion was determined by integration of the monomer versus polymer backbone resonances in the <sup>1</sup>H NMR spectrum of the crude product. After completion of the reaction, the contents of the ampules were dissolved in THF or CH<sub>2</sub>Cl<sub>2</sub>. The reaction mixture was filtered through a glass funnel with neutral alumina. The filtrate was concentrated under reduced pressure. The residuals were resolved with 5 mL of THF or CH<sub>2</sub>Cl<sub>2</sub>. This solution was added to an approximately 50-fold excess of rapidly stirred methanol. The precipitate that formed was filtered and washed with methanol. The precipitate was dried for 24 h in a vacuum oven at 60 °C. The dried samples were then analyzed by gel permeation chromatography and NMR.

## ASSOCIATED CONTENT

### Supporting Information

The Supporting Information is available free of charge on the ACS Publications website at DOI: 10.1021/acscatal.7b01079.

Experimental procedures, characterization, and figures (PDF)

Crystallographic information files for Cu(II) and Cu(I) complexes (ZIP)

## AUTHOR INFORMATION

### Corresponding Author

\*E-mail: tangy@sioc.ac.cn.

### ORCID

Yong Tang: 0000-0002-5435-9938

### Notes

The authors declare no competing financial interest.

## ACKNOWLEDGMENTS

The authors are grateful for financial support from the National Natural Science Foundation of China (21690072 and 21461162002), the Chinese Academy of Sciences (XDB 20000000), and the National Key Research and Development Program (2016YFA 0202900). We also thank Dr. S. Schaubach for assistance with editing of the English.

## REFERENCES

- (1) Wang, J.-S.; Matyjaszewski, K. *J. Am. Chem. Soc.* **1995**, *117*, 5614–5615.
- (2) Wang, J.-S.; Matyjaszewski, K. *Macromolecules* **1995**, *28*, 7901–7910.
- (3) Kato, M.; Kamigaito, M.; Sawamoto, M.; Higashimura, T. *Macromolecules* **1995**, *28*, 1721–1723.

- (4) Patten, T. E.; Xia, J.-H.; Abernathy, T.; Matyjaszewski, K. *Science* **1996**, *272*, 866–868.
- (5) Matyjaszewski, K.; Tsarevsky, N. V. *J. Am. Chem. Soc.* **2014**, *136*, 6513–6533.
- (6) Hu, R.; Leung, N. L. C.; Tang, B. Z. *Chem. Soc. Rev.* **2014**, *43*, 4494–4562.
- (7) Ran, J.; Wu, L.; Zhang, Z.; Xu, T. *Prog. Polym. Sci.* **2014**, *39*, 124–144.
- (8) Hillmyer, M. A.; Tolman, W. B. *Acc. Chem. Res.* **2014**, *47*, 2390–2396.
- (9) Zetterlund, P. B.; Thickett, S. C.; Perrier, S.; Bourgeat-Lami, E.; Lansalot, M. *Chem. Rev.* **2015**, *115*, 9745–9800.
- (10) Raffa, P.; Wever, D. A. Z.; Picchioni, F.; Broekhuis, A. A. *Chem. Rev.* **2015**, *115*, 8504–8563.
- (11) Delplace, V.; Nicolas, J. *Nat. Chem.* **2015**, *7*, 771–784.
- (12) Teator, A. J.; Lastovickova, D. N.; Bielawski, C. W. *Chem. Rev.* **2016**, *116*, 1969–1992.
- (13) Dru, D.; Baranton, S.; Bigarré, J.; Buvat, P.; Coutanceau, C. *ACS Catal.* **2016**, *6*, 6993–7001.
- (14) Boyer, C.; Corrigan, N. A.; Jung, K.; Nguyen, D.; Nguyen, T.-K.; Adnan, N. N.; Oliver, M. S.; Shanmugam, S.; Yeow, J. *Chem. Rev.* **2016**, *116*, 1803–1949.
- (15) Das, A.; Theato, P. *Chem. Rev.* **2016**, *116*, 1434–1495.
- (16) Anastasaki, A.; Nikolaou, V.; Nurumbetov, G.; Wilson, P.; Kempe, K.; Quinn, J. F. T.; Davis, P.; Whittaker, M. R.; Haddleton, D. M. *Chem. Rev.* **2016**, *116*, 835–877.
- (17) Zeng, L.; Guo, X.; He, C.; Duan, C. *ACS Catal.* **2016**, *6*, 7935–7947.
- (18) Mohapatra, H.; Kleiman, M.; Esser-Kahn, A. P. *Nat. Chem.* **2017**, *9*, 135–139.
- (19) Zoppe, J. O.; Ataman, N. C.; Mocny, P.; Wang, J.; Moraes, J.; Klok, H.-A. *Chem. Rev.* **2017**, *117*, 1105–1318.
- (20) Habaue, S.; Okamoto, Y. *Chem. Rec.* **2001**, *1*, 46–52.
- (21) Kamigaito, M.; Satoh, K. *Macromolecules* **2008**, *41*, 269–276.
- (22) Satoh, K.; Kamigaito, M. *Chem. Rev.* **2009**, *109*, 5120–5156.
- (23) Isobe, Y.; Fujioka, D.; Habaue, S.; Okamoto, Y. *J. Am. Chem. Soc.* **2001**, *123*, 7180–7181.
- (24) Lutz, J.-F.; Neugebauer, D.; Matyjaszewski, K. *J. Am. Chem. Soc.* **2003**, *125*, 6986–6993.
- (25) Miura, Y.; Satoh, T.; Narumi, A.; Nishizawa, O.; Okamoto, Y.; Kakuchi, T. *Macromolecules* **2005**, *38*, 1041–1043.
- (26) Değirmenci, İ.; Eren, Ş.; Aviyente, V.; De Sterck, B.; Hemelsoet, K.; Van Speybroeck, V.; Waroquier, M. *Macromolecules* **2010**, *43*, 5602–5610.
- (27) Patten, T. E.; Matyjaszewski, K. *Acc. Chem. Res.* **1999**, *32*, 895–903.
- (28) Johnson, R. M.; Ng, C.; Samson, C. C. M.; Fraser, C. L. *Macromolecules* **2000**, *33*, 8618–8628.
- (29) Singleton, D. A.; Nowlan, D. T.; Jahed, N.; Matyjaszewski, K. *Macromolecules* **2003**, *36*, 8609–8616.
- (30) Haddleton, D. M.; Duncalf, D. J.; Kukulj, D.; Heming, A. M.; Shooter, A. J.; Clark, A. J. *J. Mater. Chem.* **1998**, *8*, 1525–1532.
- (31) Yu, B.; Ruckenstein, E. J. *J. Polym. Sci., Part A: Polym. Chem.* **1999**, *37*, 4191–4197.
- (32) Stoffelbach, F.; Richard, P.; Poli, R.; Jenny, T.; Savary, C. *Inorg. Chim. Acta* **2006**, *359*, 4447–4453.
- (33) Iizuka, Y.; Li, Z.; Satoh, K.; Kamigaito, M.; Okamoto, Y.; Ito, J.; Nishiyama, H. *Eur. J. Org. Chem.* **2007**, *2007*, 782–791.
- (34) Bolig, A. D.; Chen, E. Y.-X. *J. Am. Chem. Soc.* **2001**, *123*, 7943–7944.
- (35) Kitaura, T.; Kitayama, T. *Macromol. Rapid Commun.* **2007**, *28*, 1889–1893.
- (36) Chen, E. Y.-X. *Chem. Rev.* **2009**, *109*, 5157–5214.
- (37) Zhang, Y.; Ning, Y.; Caporaso, L.; Cavallo, L.; Chen, E. Y.-X. *J. Am. Chem. Soc.* **2010**, *132*, 2695–2709.
- (38) Hatada, K.; Kitayama, T. *Polym. Int.* **2000**, *49*, 11–47.
- (39) Jakubowski, W.; Matyjaszewski, K. *Macromolecules* **2005**, *38*, 4139–4146.
- (40) Luo, R.; Sen, A. *Macromolecules* **2008**, *41*, 4514–4518.
- (41) Jiang, H.; Zhang, L.; Pan, J.; Jiang, X.; Cheng, Z.; Zhu, X. *J. Polym. Sci., Part A: Polym. Chem.* **2012**, *50*, 2244–2253.
- (42) Isobe, Y.; Yamada, K.; Nakano, T.; Okamoto, Y. *Macromolecules* **1999**, *32*, 5979–5981.
- (43) Isobe, Y.; Yamada, K.; Nakano, T.; Okamoto, Y. *J. Polym. Sci., Part A: Polym. Chem.* **2000**, *38*, 4693–4703.
- (44) Zhou, J.; Tang, Y. *Chem. Soc. Rev.* **2005**, *34*, 664–676.
- (45) Liao, S.-H.; Sun, X.-L.; Tang, Y. *Acc. Chem. Res.* **2014**, *47*, 2260–2272.
- (46) Zhou, J.; Tang, Y. *J. Am. Chem. Soc.* **2002**, *124*, 9030–9031.
- (47) Wang, P.; Tao, W.-J.; Sun, X.-L.; Liao, S.; Tang, Y. *J. Am. Chem. Soc.* **2013**, *135*, 16849–16852.
- (48) Kang, Q.-K.; Wang, L.; Liu, Q.-J.; Li, J.-F.; Tang, Y. *J. Am. Chem. Soc.* **2015**, *137*, 14594–14597.
- (49) Hu, J.-L.; Feng, L.-W.; Wang, L.; Xie, Z.; Tang, Y.; Li, X. *J. Am. Chem. Soc.* **2016**, *138*, 13151–13154.
- (50) Zhou, J.-L.; Wang, L.-J.; Xu, H.; Sun, X.-L.; Tang, Y. *ACS Catal.* **2013**, *3*, 685–688.
- (51) Nishiura, T.; Abe, Y.; Kitayama, T. *Polym. Bull.* **2011**, *66*, 917–923.
- (52) Thompson, E. V. *J. Polym. Sci. A-2* **1966**, *4*, 199–208.
- (53) O'Reilly, R. K.; Shaver, M. P.; Gibson, V. C.; White, A. J. P. *Macromolecules* **2007**, *40*, 7441–7452.
- (54) Xiong, H.; Xu, H.; Liao, S.-H.; Xie, Z.-W.; Tang, Y. *J. Am. Chem. Soc.* **2013**, *135*, 7851–7854.
- (55) Buschmann, H.; Scharf, H.-D.; Hoffmann, H.; Esser, P. *Angew. Chem., Int. Ed. Engl.* **1991**, *30*, 477–515.